TEXTURE-ADAPTIVE MOTHER WAVELET SELECTION FOR TEXTURE ANALYSIS

G. C. K. Abhayaratne

Dept. of Electronic Engineering
Queen Mary University of London
London E1 4NS, United Kingdom.
charith@ieee.org

I. H. Jermyn, J. Zerubia

Ariana
(INRIA/I3S joint research group)
INRIA, B.P. 93, 06902 Sophia Antipolis, France.
firstname.lastname@inria.fr

ABSTRACT

Classification results obtained using wavelet-based texture analysis techniques vary with the choice of mother wavelet used in the methodology. We discuss the use of mother wavelet filters as parameters in a probabilistic approach to texture analysis based on adaptive biorthogonal wavelet packet bases. The optimal choice for the mother wavelet filters is estimated from the data, in addition to the other model parameters. The model is applied to the classification of single texture images and mosaics of Brodatz textures, the results showing improvement over the performance of standard wavelets for a given filter length.

1. INTRODUCTION

Texture analysis plays a major role in image segmentation, classification, and descriptor extraction for content-based image retrieval. Due to its importance, texture analysis has received considerable attention in terms of both methodology and application. In one approach to texture analysis, images are first decorrelated using a signal transform, *e.g.* Gabor, ring, wedge, steerable pyramids, wavelet packets [1, 2, 3, 4, 5] or wavelet frames, before features are computed. In [3], a probabilistic texture model was developed in which the wavelet packet basis, as well as statistical features of the subbands, were treated as parameters of the model and estimated from training data. This model was extended to biorthogonal wavelet packets by considering both analysis (primal) and synthesis (dual) wavelet bases [6]. The model for biorthogonal wavelet packets reduces to that for orthogonal wavelets, as in [3], when the primal and dual bases are the same; thus we can use this model for orthogonal wavelets too.

The models of [3, 6], like most wavelet-based approaches to texture analysis, employ a single fixed mother wavelet for all textures. Thus in [3, 6], only the wavelet packet tree of the optimal subband decomposition and the statistical properties of the marginal densities for each subband were used as parameters of the texture model. However [3, 6] noted that the optimal tree for a given texture, and classification performance, both vary according to the mother wavelet used in the texture model. Previous studies have also shown that the length, number of vanishing moments, regularity, orthogonality, and degree of the impulse response shift variance of the mother wavelet contribute to the results of wavelet based applications such as image coding [7] and texture analysis [8]. Therefore, an optimal choice of mother wavelet for the representation of a given texture can be used in the feature extraction process. Similarly, in filter based methods, where a filter and a response energy measure are used as the feature extractor, optimization of filters has been used in order to achieve optimized energy separation [9, 10, 11]. All this suggests that the mother wavelet itself should be treated as a parameter of the texture models proposed in [6], and estimated, like the other parameters, from training data.

In this paper we implement this idea, treating the mother wavelet filters as parameters of the adaptive biorthogonal wavelet packet texture model. In section 2, we present the new texture model and discuss parameter estimation and classification. In section 3, we examine the parameter estimation and classification performance of the new texture model using single Brodatz textures and multi-texture Brodatz mosaics. We compare the results with those obtained using a single mother wavelet choice for all textures. We conclude in section 4.

2. TEXTURE MODEL

The purpose of this section is to review the model described in [6] and to incorporate the mother wavelet parameters. The model in [6] starts from a general translation invariant Gaussian distribution. The marginalized Gaussian distribution on an image region is then derived, and shown to be tractable if the original covariance lies in a certain class of operators. This class consists of those operators that are diagonal in at least one wavelet packet basis. The model is thus parameterized by a dyadic partition of the Fourier domain, T, which in conjunction with a mother wavelet de-

Dr. Abhayaratne would like to thank ERCIM for support during the performance of this work.

fines a wavelet packet basis, and a function f that assigns to each element of the partition (*i.e.* each subband), its variance. In [3], it is shown that exact MAP estimates of these parameters can be learned from samples of a texture using an efficient depth-first search algorithm on the space of dyadic partitions. The result is a model in which the basis adapts to the structure inherent in the texture according to a criterion derived from the texture model itself, rather than introduced on an *ad hoc* basis.

The model in [6] also implicitly includes the mother wavelet $W = (P, U)$, where P and U are the filters for the prediction and update steps in the lifting realization of wavelets. These lifting steps define the primal and dual wavelets, respectively. In the new model, these filters are promoted to parameters. The new model thus takes the form

$$\mathrm{P}(I|f,T,W) = \prod_{\alpha\in T}\left[\left(\frac{f_\alpha}{\pi}\right)^{\frac{N_\alpha}{2}} e^{-f_\alpha \sum_{i\in\alpha} w_{a_{\alpha,i}} w_{s_{\alpha,i}}}\right]$$

where I is the image; α indexes the subbands of T; f_α is the value of f on subband α; i indexes the wavelets within each subband; $w_{a_{i,\alpha}}$ and $w_{s_{i,\alpha}}$ are the (α, i) coefficients in the analysis and synthesis wavelet packet bases derived from W; and N_α is the number of pixels in the subband α. We refer the reader to [6] for the relationship between the lifting weights P, U and the primal-dual wavelet pair.

2.1. Texture model training

MAP estimates of the parameters for a given texture are found by examining the probability of the parameters given a set of images $d = \{I_n\}$ of the texture:

$$\mathrm{P}(f,T,W|d) \propto \mathrm{P}(d|f,T,W)\mathrm{P}(f|T,W)\mathrm{P}(T|W)\mathrm{P}(W)$$

We choose $\mathrm{P}(f|T,W)$ to be Jeffrey's ignorance prior. We choose the probability $\mathrm{P}(T|W) = Z^{-1}(\beta)e^{-\beta\sum_{t\in Q(T)} N_t}$, where $Q(T)$ is the quadtree naturally related to the partition; t is a vertex in this tree; and $N_t \propto 4^{-l(t)}$, where $l(t)$ is the depth of vertex t in the tree, is the size of the region of the Fourier domain corresponding to vertex t. The parameter β controls how severely the distribution penalizes large decompositions. We choose the wavelet prior $\mathrm{P}(W)$ to be uniform. The MAP estimate of f for fixed T and W is of course given by

$$\hat{f}_\alpha = \frac{N_\alpha}{2\sum_{i\in\alpha}|w_{a_{i,\alpha}} w_{s_{i,\alpha}}|}$$

A depth-first search through the space of dyadic decompositions allows us to find the MAP estimate $\hat{T}$ for T efficiently for a fixed wavelet choice W. Finally, the MAP estimate for W is found as follows:

$$\hat{W} = (\hat{P},\hat{U}) = \arg\max_{(P\in\mathcal{P},U\in\mathcal{U})} \mathrm{P}(d|\hat{f},\hat{T},(P,U)),$$

where $\mathcal{P}$ and $\mathcal{U}$ are the sets of choices for the lifting filters P and U. Note that $\hat{T}$ is a function of (P,U), and that $\hat{f}$ is a function of $\hat{T}$ (hence (P,U)), and (P,U).

2.2. Classification

In order to classify pixels, we use an undecimated wavelet decomposition, and consider the following approximation to the exact probability distribution for the texture on an arbitrary region R:

$$\mathrm{P}(I_R|f,T,W) = \prod_{\alpha\in T}\prod_{x\in R}\left[\left(\frac{f_\alpha}{\pi}\right)^{\frac{1}{2M_\alpha}} e^{-\frac{f_\alpha}{M_\alpha}\sum_{i\in\alpha} w_{a_{\alpha,x}} w_{s_{\alpha,x}}}\right]$$

where $M_\alpha = 4^{l(\alpha)}$ is the redundancy factor for subband α in the undecimated transform. The class of a pixel, $\lambda(x)$, is then estimated from

$$\hat{\lambda}(x) = \arg\max_{l\in L} \mathrm{P}(I_{V(x)}|\lambda_{V(x)} = l)$$

where $V(x)$ is a set of neighbours of pixel x.

3. SIMULATION RESULTS

In this paper, we evaluate the proposed model by focusing on finding the optimal mother wavelet for a given texture from a finite set of mother wavelet choices. We show an example using interpolating wavelets with P and U filters of length 4. In general, one can define the interpolating filter template of length 4, denoted Int_4, by

$$\mathrm{Int}_4 = \begin{pmatrix} -v & \frac{1}{2}+v & \frac{1}{2}+v & -v \end{pmatrix}$$

We choose $v = (k-1)/64$ for $k \in [1, 2, \ldots, 17]$. The resulting interpolation functions are shown in table 1. The choices 1 and 5 correspond to the classical linear and cubic interpolation functions, respectively. We define a set of interpolating wavelets by choosing the interpolating templates in the table as P and U filters. We denote such wavelets (k-l), where k and l are the indices for the chosen P and U filters, respectively. For example, the well-known biorthogonal wavelets (2,2), (4,2), (2,4) and (4,4) (using the vanishing moment pair notation) correspond to the wavelet choices (1-1), (5-1), (1-5) and (5-5) in the table.

3.1. Parameter Estimation

We compute $\mathrm{P}(d|\hat{f},\hat{T},(P,U))$ for each of the mother wavelet choices (k-l) using the 17 interpolating functions shown in table 1. This yields 289 choices of mother wavelet filters to be used in parameter estimation experiments. In Fig. 3.1, we show the logarithms of the probabilities for the different

k	Int_4
1	$\begin{pmatrix} 0 & \frac{1}{2} & \frac{1}{2} & 0 \end{pmatrix}$
2	$\begin{pmatrix} -\frac{1}{64} & \frac{33}{64} & \frac{33}{64} & -\frac{1}{64} \end{pmatrix}$
3	$\begin{pmatrix} -\frac{1}{32} & \frac{17}{32} & \frac{17}{32} & -\frac{1}{32} \end{pmatrix}$
4	$\begin{pmatrix} -\frac{3}{64} & \frac{35}{64} & \frac{35}{64} & -\frac{3}{64} \end{pmatrix}$
5	$\begin{pmatrix} -\frac{1}{16} & \frac{9}{16} & \frac{9}{16} & -\frac{1}{16} \end{pmatrix}$
6	$\begin{pmatrix} -\frac{5}{64} & \frac{37}{64} & \frac{37}{64} & -\frac{5}{64} \end{pmatrix}$
7	$\begin{pmatrix} -\frac{3}{32} & \frac{19}{32} & \frac{19}{32} & -\frac{3}{32} \end{pmatrix}$
8	$\begin{pmatrix} -\frac{7}{64} & \frac{39}{64} & \frac{39}{64} & -\frac{7}{64} \end{pmatrix}$
9	$\begin{pmatrix} -\frac{1}{8} & \frac{5}{8} & \frac{5}{8} & -\frac{1}{8} \end{pmatrix}$
10	$\begin{pmatrix} -\frac{9}{64} & \frac{41}{64} & \frac{41}{64} & -\frac{9}{64} \end{pmatrix}$
11	$\begin{pmatrix} -\frac{5}{32} & \frac{21}{32} & \frac{21}{32} & -\frac{5}{32} \end{pmatrix}$
12	$\begin{pmatrix} -\frac{11}{64} & \frac{43}{64} & \frac{43}{64} & -\frac{11}{64} \end{pmatrix}$
13	$\begin{pmatrix} -\frac{3}{16} & \frac{11}{16} & \frac{11}{16} & -\frac{3}{16} \end{pmatrix}$
14	$\begin{pmatrix} -\frac{13}{64} & \frac{45}{64} & \frac{45}{64} & -\frac{13}{64} \end{pmatrix}$
15	$\begin{pmatrix} -\frac{7}{32} & \frac{23}{32} & \frac{23}{32} & -\frac{7}{32} \end{pmatrix}$
16	$\begin{pmatrix} -\frac{15}{64} & \frac{47}{64} & \frac{47}{64} & -\frac{15}{64} \end{pmatrix}$
17	$\begin{pmatrix} -\frac{1}{4} & \frac{3}{4} & \frac{3}{4} & -\frac{1}{4} \end{pmatrix}$

Table 1. Different choices for length 4 interpolation function templates.

(k-l) mother wavelets choices for the textures Raffia, Herring, Wool and Grass (brightness is proportional to the log probability).

The optimal mother wavelets $\hat{W}$ for each of the test textures were found to be (4-11), (4-12), (6-6) and (4-14), respectively. Interestingly, none of the above choices corresponds to the commonly used wavelet filters. The parameters T and f are estimated as described earlier. They are shown graphically and compared with the corresponding power spectra in Fig. 2. The brightness of each subband is proportional to $1/f_\alpha$.

3.2. Classification

We present the classification performance of the texture-adaptive optimal biorthogonal mother wavelet packet model using single texture images and texture mosaic images. Fig. 3 shows the classification maps for four textures, classified using all four trained texture models on each of the single texture images. The percentages of misclassified pixels are listed in table 2. Similarly, Fig. 4 shows the classification performance for test mosaics, M1, M2, M3 and M4, made of 4 test textures. The percentages of misclassified pixels are listed in table 3.

As can be seen from the tables, using the optimal mother wavelet for modelling the textures results in better classification performance than using fixed mother wavelets involving lifting templates of length 4, *i.e.* (4,4), (4,2) and (2,4).

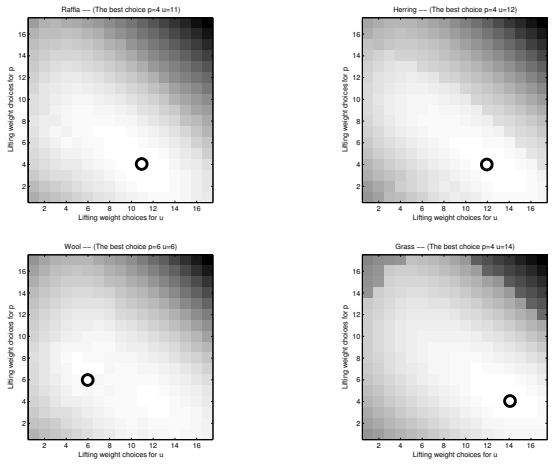

Fig. 1. Log probabilities for different choices of P and U lifting weights for different textures. Increasing brightness corresponds to increasing probability. Top row: Raffia ($\hat{W}$ = (4-11)) and Herring ($\hat{W}$ = (4-12)); Bottom Row: Wool ($\hat{W}$ = (6-6)) and Grass ($\hat{W}$ = (4-14)).

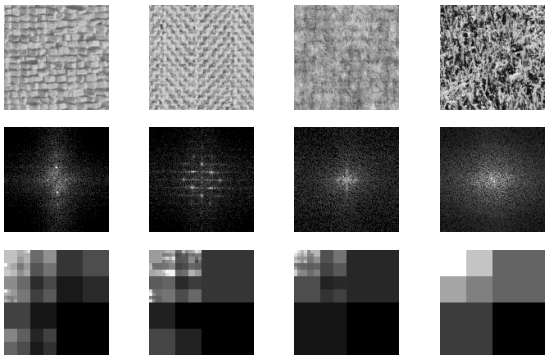

Fig. 2. Parameter estimation. Row 1: textures Raffia, Herring, Wool, and Grass; row 2: their power spectra; row 3: their estimated parameters using the optimal mother wavelet.

	T1	T2	T3	T4	Average
Optimal	0.13	1.41	9.21	9.98	5.18
(2,4)	0.19	1.79	13.11	11.91	6.75
(4,2)	0.01	4.80	7.16	11.97	5.98
(4,4)	0.18	1.89	15.49	10.02	6.90

Table 2. Percentages of misclassified pixels (Single).

4. CONCLUSION

In this paper, we have incorporated the choice of mother wavelet into an adaptive probabilistic texture model based

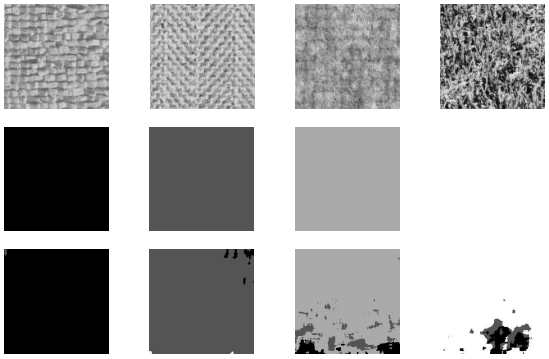

Fig. 3. Classification results. Row 1: Raffia, Herring, Wool, and Grass; row 2: ground truth; rows 3: classification map using the optimal mother wavelet.

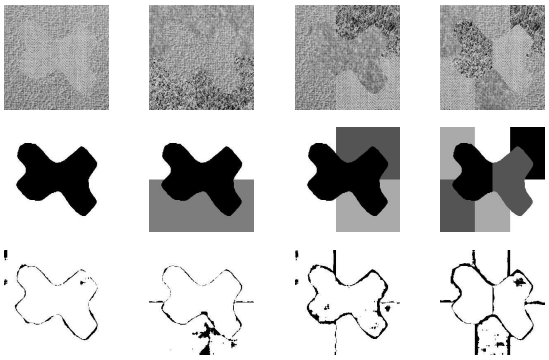

Fig. 4. Classification results. Row 1: mosaics M1, M2, M3, and M4; row 2: ground truth; rows 3: misclassified pixels (in black) using the optimal mother wavelet.

on biorthogonal wavelets. The optimal mother wavelet for a given texture is given by the mother wavelet that maximizes the MAP probability of the derived biorthogonal wavelet packet texture model. We have shown examples of the best choices for prediction and update lifting weights using length 4 lifting templates for four different textures. The optimal lifting weight choices result in better classification performance than the standard (4,4), (2,4) and (4,2) wavelets, all of which include length 4 prediction and/or update lifting templates. Future work includes optimization of the mother wavelet filter coefficients for a range of different wavelet classes.

	M1	M2	M3	M4	Average
Optimal	2.79	4.76	6.86	8.93	5.84
(2,4)	2.67	4.72	6.78	10.96	6.28
(4,2)	2.83	5.77	6.06	9.18	5.96
(4,4)	2.83	7.60	6.07	10.62	6.78

Table 3. Percentages of misclassified pixels (Mosaics).

References

[1] T. Chang and C.-C. J. Kuo, "Texture analysis and classification with tree structured wavelet transform," *IEEE Trans. Image Processing*, vol. 2, no. 4, pp. 429–441, 1993.

[2] A. Laine and J. Fan, "Texture classifiction by wavelet packet signatures," *IEEE Trans. Patt. Anal. Mach. Intell.*, vol. 15, no. 11, pp. 1186–1190, 1993.

[3] K. Brady, I. H. Jermyn, and J. Zerubia, "Texture analysis: An adaptive probabilistic approach," in *Proc. IEEE ICIP*, 2003, vol. 2, pp. 1045–1048.

[4] N. Rajpoot, "Local discriminant wavelet packet basis for texture classification," in *Wavelets: Applications in Signal and Image Processing X*, 2003, vol. Proc. SPIE 5207, pp. 774–783.

[5] M. Acharyya and M. K. Kundu, "Adaptive basis selection for multi texture segmentation by m-band wavelet packet frames," in *Proc. IEEE ICIP*, 2001, vol. 1, pp. 622–625.

[6] G. C. K. Abhayaratne, I. H. Jermyn, and J. Zerubia, "Texture analysis using adaptive biorthogonal wavelet packets," in *Proc. IEEE ICIP*, 2004, vol. 1, pp. 1197–1200.

[7] M. D. Adams and F. Kossentini, "Reversible integer-to-integer wavelet transforms for image compression: Performance evaluation and analysis," *IEEE Trans. Image Processing*, vol. 9, no. 6, pp. 1010–1024, 2000.

[8] D. M. Rackov A. Mojsilovic, M. V. Popovic, "On the selection of an optimal wavelet basis for texture characterization," *IEEE Trans. Image Processing*, vol. 9, no. 12, pp. 2043–2050, 2000.

[9] T. Randen and J. H. Husoy, "Texture segmentation using filters with optimized energy seperation," *IEEE Trans. Image Processing*, vol. 8, no. 4, pp. 571–582, 1999.

[10] T. Randen and J. H. Husoy, "Optimal filter-bank design for multiple texture discrimination," in *Proc. IEEE ICIP*, 1997, vol. 2, pp. 215–218.

[11] F. Nergard and T. Randen, "Optimization of spatial filters for image texture feature seperation by simulated annealing," in *NORSIG*, 1996, pp. 251–254.